



HAL
open science

Out of equilibrium anomalous elastic response of a water nano-meniscus

Simon Carpentier, Mario Rodrigues, Miguel V Vitorino, Luca Costa,
Elisabeth Charlaix, Joel Chevrier

► **To cite this version:**

Simon Carpentier, Mario Rodrigues, Miguel V Vitorino, Luca Costa, Elisabeth Charlaix, et al.. Out of equilibrium anomalous elastic response of a water nano-meniscus. Applied Physics Letters, 2015, 107 (20), pp.204101. 10.1063/1.4935836 . hal-01876143

HAL Id: hal-01876143

<https://hal.science/hal-01876143>

Submitted on 18 Sep 2018

HAL is a multi-disciplinary open access archive for the deposit and dissemination of scientific research documents, whether they are published or not. The documents may come from teaching and research institutions in France or abroad, or from public or private research centers.

L'archive ouverte pluridisciplinaire **HAL**, est destinée au dépôt et à la diffusion de documents scientifiques de niveau recherche, publiés ou non, émanant des établissements d'enseignement et de recherche français ou étrangers, des laboratoires publics ou privés.

Out of equilibrium anomalous elastic response of a water nano-meniscus

Simon Carpentier,^{1,2} Mario S. Rodrigues,³ Miguel V.Vitorino,³

Luca Costa,⁴ Elisabeth Charlaix,^{1,5} and Joël Chevrier^{1,2}

¹*Univ. Grenoble Alpes, F-38000 Grenoble, France*

²*CNRS, Inst NEEL, F-38042 Grenoble, France*

³*Uniservity of Lisboa, Faculty of Sciences, BioISI-Biosystems & Integrative Sciences Institute, Campo Grande, Lisboa, Portugal*

⁴*ESRF, The European Synchrotron, 71 Rue des Martyrs, 38000 Grenoble, France*

⁵*CNRS, LIPhy, Grenoble, F-38402, France*

We report the observation of a transition in the dynamical properties of water nano-meniscus which dramatically change when probed at different time scales. Using a AFM mode that we name Force Feedback Microscopy, we observe this change in the simultaneous measurements, at different frequencies, of the stiffness G' (N/m), the dissipative coefficient G'' (kg/sec) together with the static force. At low frequency we observe a negative stiffness as expected for capillary forces. As the measuring time approaches the microsecond, the dynamic response exhibits a transition toward a very large positive stiffness. When evaporation and condensation gradually lose efficiency, the contact line progressively becomes immobile. This transition is essentially controlled by variations of Laplace pressure.

Visco-elastic properties of water nanobridges[1] at very different time scales, have never been investigated despite ubiquitous presence of capillarity. Associated forces are among the most intense at nanoscales with important consequences in soils and granular media. Interest in dynamical properties is immediately raised if one considers interacting surfaces with roughness scales down to nanometer. Even at moderate speeds, such as $v=1\text{m/s}$, characteristic times of surface interaction down to microsecond appear in these conditions. Our measurements approaching these time scales, further strengthen the relevance of the dynamical properties to describe how real surfaces interact and are certainly of crucial importance in numerous AFM experiments [2]. We here report measurements of dynamical properties of a water nanobridge for a continuous range of the surface gap and a frequency bandwidth up to 0.1 MHz. We identify two regimes: one is the thermodynamical equilibrium; the second is out of equilibrium. Evaporation and condensation of water molecules between the liquid and the gas phase ensures that the nano-meniscus curvature is the one at thermodynamical equilibrium($2H=-1/r_k$) where $2H$ is the water bridge curvature and r_k is the Kelvin radius. At time short enough, molecule exchanges between the liquid and the gas phase are no longer efficient and the water nanobridge is led to acquire a constant volume. The liquid bridge relaxation time is the time needed for the bridge to adapt its shape as required by thermodynamical equilibrium, when its length h is abruptly changed by δh . This is controlled by molecular transport through diffusion mechanisms in gas phase. This relaxation time τ can be estimated as in SFA context, see Ref.[3].

$$\tau = 2\gamma\rho r^2 \ln(R/\rho)/P_{\text{sat}} r_k^2 D \quad (1)$$

D is the diffusion coefficient of water molecules in air ($D=0.282\text{cm}^2/\text{sec}$ from Ref.[4]). ρ is the bridge azimuthal radius, r , its meridional radius. P_{sat} is the saturated vapor pressure, R is the typical scale of the overall

system and γ the surface tension of the vapor liquid interface. In our experimental conditions, with a Kelvin radius r_k of about 12nm, the characteristic time is found to be around $\tau=10^{-6}$ second. As $\omega/2\pi$ increases from 300Hz to 114kHz, in our experiment, $\omega\tau$ evolves from $2\cdot 10^{-3}$ to 0.7. At $\omega\tau=2\cdot 10^{-3}$, the liquid nanobridge should be observed at thermodynamical equilibrium. At $\omega\tau=0.7$, $\omega/2\pi=114\text{kHz}$, this time τ is too short for the thermodynamical equilibrium to settle during oscillation. We shall therefore consider an extreme regime with constant volume when dealing with analysis of experiments performed at these high frequencies.

Using the AFM mode that we name Force Feedback Microscopy (FFM), we have measured simultaneously the static force, the interaction stiffness G' and the associated dissipation G'' at different frequencies. As described in Fig.1.(a), the FFM used to perform this experiment is based on a homemade AFM setup with optical fiber [5]. These three simultaneous measurements are done using a single nanotip-microlever system, with excitation frequency varied from 300Hz up to 114kHz. During FFM experiments, a feedback force is applied in real time to the tip so that it cancels the force due to the surface (this suppresses the “jump to contact” observed in classical AFM force-approach curve). The total force applied to the tip is then equal to zero and the tip remains immobile. To apply this force in real time, a piezoelement simply changes the DC position of the clamped end part of the microlever. This measured displacement multiplied by the lever stiffness k results in the static tip/surface force measurement. Measured on this basis [6, 7], the static force is reported in Fig.1.(b). Both the tip radius and the Kelvin radius, r_k are then estimated. The minimum force is roughly $-4\pi\gamma R$, which leads to R close to 14nm, see more details in Ref.[8]. The slope of the force versus distance as the AFM tip is retracted, gives $r_k=12\text{nm}$ [9, 10]. As shown in Fig.1.(a), a nanometric oscillation is imposed to the tip. Measure of the tip amplitude and the associated phase shift leads to

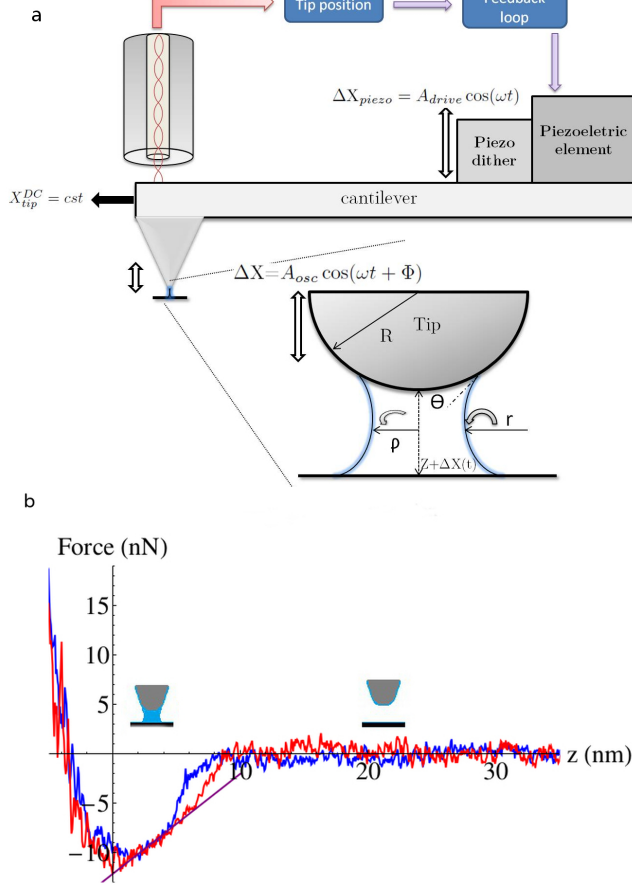


Figure 1. (a) Description of the FFM measurement strategy. The DC tip position is a constant. This is due to real time application of a feedback force determined through a control loop after measurement of the tip position. Piezodither enforces an AC tip oscillation with 1 nm of free oscillation amplitude. A_{osc} and Φ are the measured quantities. (b), Static force measured between a brand new silicon AFM tip and a plane silicon sample during approach (blue) and retract (red) by FFM in presence of a capillary bridge. The linear behavior is fitted using the approximate solution given by J.Crassous et al. in Ref.[8] with $R=14\text{nm}$ and $r_k=12\text{nm}$.

the determination of the stiffness interaction and the associated dissipation following these linear equations (see details in Ref.[11]):

$$G' = F_r [n \cos(\Phi) - \cos(\Phi_\infty)] \quad (2)$$

$$G'' = \frac{F_r}{\omega} [-n \sin(\Phi) + \sin(\Phi_\infty)] \quad (3)$$

Φ is the phase shift between excitation at the lever clamped end and the tip oscillation. n is the normalized amplitude of tip vibration i.e. the measured amplitude at

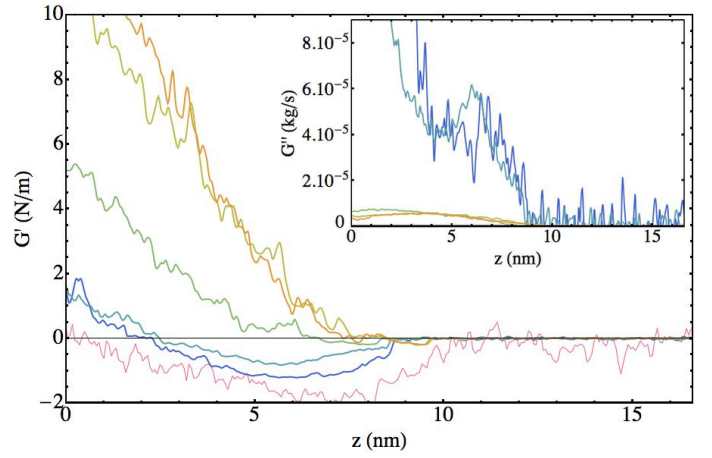


Figure 2. From blue to orange curves (respectively 300 Hz, 1 kHz, 44 kHz, 94 kHz and 114 kHz) show interaction stiffness, G' versus tip surface distance as deduced from experimental measurements using Eq.2. Red curve is the negative of the numerical derivative of the measured static force as the tip is pulled away from the surface. Inset: $G''(\text{kg/sec})$ result from Eq.3. It characterizes the mechanical energy dissipation increase during tip oscillation due to the capillary bridge. G'' at high frequencies is distinctively decreased as compared to G'' at low frequencies. Dissipation when in the thermodynamical equilibrium is clearly much higher.

distance z divided by the measured amplitude when tip is far away from the surface. At large distance $n=1$. In the experimental environment used (normal conditions in air), values of F_r and Φ_∞ are directly obtained from the system transfer function when the tip is far from the surface.

$$F_r = [(k - m\omega^2)^2 + c^2\omega^2]^{1/2} \quad (4)$$

$$\Phi_\infty = \arctan[(c/m)\omega/(\omega^2 - \omega_0^2)] \quad (5)$$

In the used frequency range with first resonance at 74,330kHz, a single mode description of the lever dynamics is sufficient. The stiffness of the lever k is obtained from measurement of the Brownian motion. The damping coefficient c and ω_0 (and therefore m) are obtained from lever transfer function measurement when the tip is far from the surface. F_r and Φ_∞ determined using this method are inserted in Eq.2 and 3 to obtain G' and G'' from n and Φ . In Fig.2, $k=2 \text{ N/m}$, $c=2.49 \cdot 10^{-8} \text{ kg/sec}$ and $\omega_0/2\pi=74,330\text{kHz}$.

Fig.2 shows that the visco-elastic coefficients exhibit a strong variation as the excitation frequency is varied over close to 3 orders of magnitude: G' varies from -1N/m up to 10N/m (therefore from negative to positive). The positive stiffness measured at high frequency, $G'=+10\text{N/m}$ is a very high interaction stiffness in AFM field. It is surprisingly observed associated to water and to an intense attractive static force close to 10nN . From this apparent

positive stiffness, although only surface effects due to the nano-meniscus are at work, an effective Young modulus E can be formally deduced: $E = G'z/\pi r_b$. It is in the range 0.1-1 GigaPa and increases as the tip moves closer to the surface.

At $\omega/2\pi=300\text{Hz}$, the measured interaction stiffness G' corresponds to the numerical derivative of the static force versus distance (i.e. the derivative of the red curve in Fig.1(b)). Here $\omega\tau \ll 1$ and the water nanobridge appears in thermodynamical equilibrium. However, the gradual increase of the excitation frequency leads to an important increase of the interaction stiffness, which finally becomes positive at all investigated distances [12]. The high frequency regime with positive and high stiffness is therefore an out of equilibrium behavior of the water droplet. As determined by use of Eq. 1, an estimate of the bridge relaxation time τ is 10^{-6}sec : the water molecule exchange between liquid and gas diminishes as the frequency increases toward 1MHz. This ultimately leads to a regime with a water nanobridge that has a constant volume. With this hypothesis of constant volume at high frequency, we analyze the observed positive stiffness G' due to the water nano-meniscus properties. This in fact follows analysis of Lambert et al in Ref.[13] produced for far larger water bridge (millimeter range). Equation 6 shows the expression of the total force due to the water nano-meniscus on the tip:

$$F = 2\pi r_b \gamma \sin(\theta) - 2H\pi r_b^2 \gamma \quad (6)$$

The force decomposes in two terms. The first term of Eq.6 is due to the tension associated to the contact line whereas the second is due to the Laplace pressure. γ is the water surface tension, $2\pi r_b$ the length of the circular contact line (or triple line), ($2H=1/\rho-1/r$) and θ , the angle between the water bridge and the surfaces. At thermodynamic equilibrium ($\omega\tau \ll 1$) with efficient evaporation condensation processes, whatever the tip surface distance and the oscillation amplitude, H is a negative constant. The pressure inside the bridge then does not change, and the contact line moves to accommodate this constrain of constant curvature as the tip surface distance is varied. During shortening of the bridge ($\delta h < 0$), the radius r_b increases as a result of the bridge spreading: the resulting stiffness $\delta F/\delta h$ is negative as observed experimentally. At $\omega\tau \gg 1$, we consider that the nanobridge volume remains constant. If the contact line does not move, the radius r_b is constant and the curvature increases ($H < 0$) as described in Fig.3(a). The second term in the force then provides a contribution to stiffness that is:

$$\frac{\delta F}{\delta h} = -2\pi r_b^2 \gamma \frac{\delta H}{\delta h} \quad (7)$$

This $\delta F/\delta h$ is then a positive contribution, which explains the origin of the positive stiffness experimentally observed.

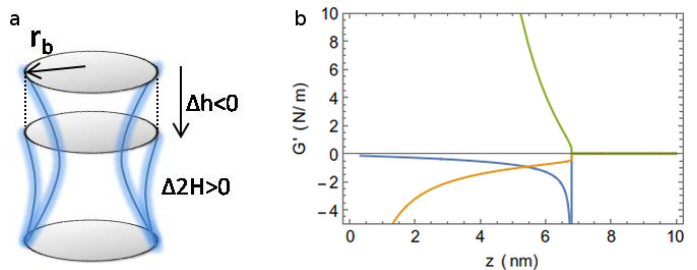


Figure 3. (a), evolution of the capillary bridge shape as the gap decreases at constant volume and at locked contact line. (b), results from numerical calculation, reproduce the key experimental features obtained using Force Feedback Microscopy at different frequencies. At low frequency (blue curve), the signature of the thermodynamical equilibrium is again obtained with a negative stiffness at all distances. At high frequency oscillation (green curve), the water nanobridge is at constant volume and the contact line is immobile. A positive stiffness is obtained like in experimental results. It is however significantly above all measured stiffnesses for which, at $\omega\tau=0.7$, contact line mobility is reduced but certainly far from zero. The orange curve represents a regime at constant volume, but with a contact line free to move. It leads to a negative stiffness. This regime, which implies a curvature only marginally varying, cannot explain the experimental observations at high frequency.

A numerical calculation of the stiffness G' in the three extreme regimes (thermodynamical equilibrium, constant volume with locked contact line or free to move contact line) is reported in Fig.3(b).

Finally as shown in inset of Fig.2, $G''(\text{kg}/\text{sec})$, the dissipative part of the linear response, is found to decrease as the excitation frequency increases and as G' severely increases. This leads us to conclude that this change of G'' is also determined by the contact line behavior. A mobile contact line on the AFM tip then appears to be associated to an important dissipation. As mobility of the contact line decreases, this channel of energy dissipation closes and G'' diminishes accordingly. Although only surface effects are here at work, G'' can be formally analyzed as an apparent volume viscosity: $G'' \propto \eta R$, where $R=14\text{nm}$ is the tip size. In that case, with a typical $G''=10^{-5} \text{ kg}/\text{sec}$ here measured and taken equal to ηR , η is in the range $10^2-10^3 \text{ Pa}\cdot\text{sec}$. This is orders of magnitude above $\eta=10^{-3} \text{ Pa}\cdot\text{sec}$, the bulk value of water viscosity(Ref.[14, 15]).

In conclusion, for the first time, two different viscoelastic regimes in dynamical properties of a water nanobridge are measured. The major result is that, despite the fact that the static interaction between surfaces associated to capillary bridges is always attractive, an apparent and highly positive stiffness appears at the nanoscale when the two surfaces interact with a short characteristic time, whereas, the friction measured in same conditions, is found strongly reduced. A description can be proposed to simultaneously explain these

results. Contrary to the situation at thermodynamical equilibrium with condensation and evaporation, in the out of equilibrium regime, any displacement of the line can only be ensured by a flow in the nanodroplet. The sticky boundary condition leads to a diverging shear velocity as the water film thickness goes to zero close to the triple line. In this situation, moving the line becomes extremely difficult. Indeed, we observe in the diminution of G'' , at high frequencies a drop of the line mobility. In this case, at constant volume, there is then no alternative: the curvature of the nano-meniscus must change, which we observe in the increase of G' .

The frequency ranges in our experiments are the ones used to operate AFM in dynamical mode. Results presented here will certainly have to be considered in the daily analysis of dynamic mode AFM experiences when

a water nanobridge is present. Due the importance of the observed changes in effective visco-elastic properties of water at nanoscale, this conclusion is certainly not limited to AFM but opens a broader perspective, as capillary bridges are now known to be important in surface interactions not only at different scales but also at different time scales.

ACKNOWLEDGMENTS

Mario S. Rodrigues and Miguel V. Vitorino acknowledge financial support from Fundação para a Ciência e Tecnologia, grants SFRH/BPD/69201/2010 and PD/BD/105975/2014 respectively.

-
- [1] William Thomson. 4. on the equilibrium of vapour at a curved surface of liquid. *Proceedings of the Royal Society of Edinburgh*, 7:63–68, 1872.
 - [2] Elisa Riedo, Francis Lévy, and Harald Brune. Kinetics of capillary condensation in nanoscopic sliding friction. *Physical review letters*, 88(18):185505, 2002.
 - [3] Jérôme Crassous. *Etude d'un pont liquide de courbure nanométrique: propriétés statiques et dynamiques*. PhD thesis, 1995.
 - [4] Edward Lansing Cussler. *Diffusion: mass transfer in fluid systems*. Cambridge university press, 2009.
 - [5] D Rugar, HJ Mamin, and Peter Guethner. Improved fiber-optic interferometer for atomic force microscopy. *Applied Physics Letters*, 55(25):2588–2590, 1989.
 - [6] Mario S Rodrigues, Luca Costa, Joël Chevrier, and Fabio Comin. Why do atomic force microscopy force curves still exhibit jump to contact? *Applied Physics Letters*, 101(20):203105, 2012.
 - [7] Luca Costa, Mario S Rodrigues, Simon Carpentier, Pieter Jan van Zwol, Joël Chevrier, and Fabio Comin. Comparison between atomic force microscopy and force feedback microscopy static force curves. *arXiv preprint arXiv:1306.2775*, 2013.
 - [8] Jérôme Crassous, Matteo Ciccotti, and Elisabeth Charlaix. Capillary force between wetted nanometric contacts and its application to atomic force microscopy. *Langmuir : the ACS journal of surfaces and colloids*, 27(7):3468–73, April 2011.
 - [9] Mika M Kohonen and Hugo K Christenson. Capillary condensation of water between rinsed mica surfaces. *Langmuir*, 16(18):7285–7288, 2000.
 - [10] This measured value of r_k is higher than expected based on vapor pressure. We have not controlled the hygrometry level during numerous experiments. We estimate an average value of hygrometry of 50 per cent. This would lead to a Kelvin radius r_k clearly smaller than 5nm. A hygrometry level close to 99 per cent is required to observe a Kelvin radius of about 12nm. This is certainly not our case. It is however known that with no special treatment of the used silicon surfaces, large Kelvin radii are commonly observed, see previous reference. $r_k=12\text{nm}$ is the value we have used to determine the characteristic time.
 - [11] Mario S Rodrigues, Luca Costa, Joël Chevrier, and Fabio Comin. System analysis of force feedback microscopy. *Journal of Applied Physics*, 115(5):054309, 2014.
 - [12] At $w=44\text{kHz}$ and above, the measured stiffness reaches values between 6N/m and 10N/m. Direct contact between the tip and a hard surface with Pauli repulsion at work, could be responsible for such a high stiffness. All curves presented in Fig. 2 have been measured during pulling the tip away from the surface. At all frequencies, we used exactly the same experimental conditions: tip control, lever oscillation amplitude, and overall time to acquire data along a complete approach/retract force curve. We simultaneously measured the static force and the dynamic response, so that we know at each point, what is the DC tip position in the static force curve shown in Fig. 1(b). The same conditions, at identical tip surface distance, with comparable oscillation amplitude, lead to a negative stiffness at low frequencies and to a positive one at high frequency. We then conclude that this increase is a direct consequence of the water bridge dynamical properties and that at high frequencies, the water bridge becomes much stiffer.
 - [13] J-B Valsamis, Massimo Mastrangeli, and Pierre Lambert. Vertical excitation of axisymmetric liquid bridges. *European Journal of Mechanics-B/Fluids*, 38:47–57, 2013.
 - [14] Using small-amplitude AFM based technique, variations of dynamical properties of a confined liquid such as a comparable increase of the stiffness, have been reported in Ref.15. This leads authors to conclude that bulk properties of water are changed by confinement close to a surface. These reports are related to change in molecular structure of liquid layers whereas in our case, the nano-meniscus behavior is the key. In Ref.15, the tip is immersed into the bulk liquid. There is no nano-meniscus due to a gas-liquid interface. The strong reported variations occur when the tip-surface distance is below 1nm, as in our case the relevant separations are between 1nm and 10nm.
 - [15] Shah H Khan, George Matei, Shivprasad Patil, and Peter M Hoffmann. Dynamic solidification in nanoconfined water films. *Physical review letters*, 105(10):106101, 2010.